BOLETIN DE LA SOCIEDAD ESPAÑOLA DE
Cerámica y Vidrio
www.elsevier.es/bsecv

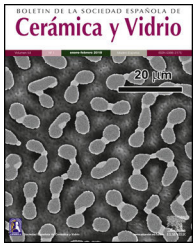

Improvement of mechanical and dielectric properties of porcelain insulators using economic raw materials

Khaled Belhouchet[a,*], *Abdelhafid Bayadi*[a], *Hocine Belhouchet*[b], *Maximina Romero*[c]

[a] *Laboratory of Electrical Engineering, University of Ferhat Abbas Setif 1, Setif 19000, Algeria*
[b] *Non Metallic Materials Laboratory, Institute of Optics and Precision Mechanics, University of Ferhat Abbas Setif 1, Setif 19000, Algeria*
[c] *Group of Glass and Ceramic Materials, Eduardo Torroja Institute for Construction Sciences, CSIC, C/ Serrano Galvache 4, 28033 Madrid, Spain*

ARTICLE INFO

Article history:
Received 29 December 2017
Accepted 22 May 2018
Available online 5 July 2018

Keywords:
Kaolin (DD2)
Quartz
Recycled waste glass
Porcelain
Vickers hardness
Dielectric properties

ABSTRACT

The present study is aimed to develop porcelain from locally available raw materials. This porcelain was prepared from the mixture of kaolin, quartz, feldspar, and recycled waste glass. In this work, the expensive K-feldspar was substituted by recycled waste glass derived from broken car glass. The effects of recycled waste glass in partial replacement of K-feldspar for porcelain are discussed. Experimental results showed significant effects of recycled waste glass substitution and sintering temperature on physical properties. Furthermore, the microstructure observation indicated that the replacement of K-feldspar by the recycled waste glass indicates the reducing firing temperature 200 °C was achieved by 30 wt% glass addition. Moreover, experimental investigations showed excellent mechanical (micro-hardness) and insulating properties (dielectric strength) of the prepared porcelain when compared to that of traditional porcelain insulators. The Vickers micro-hardness found an increase with both glass addition and sintering temperature. Dielectric constant (ε'), dielectric loss tangent ($\tan\delta$) and loss factor (ε'') were measured at different frequencies. The results reveal that glass addition enhances the dielectric properties of the samples fired at 1100 °C. Finally, the best results of phase angle were obtained ~(−89.2°) for this porcelain. These results prove that our prepared insulator is a dielectric capacitor.

Mejora de las propiedades mecánicas y dieléctricas de los aislantes de porcelana mediante el uso de materias primas económicas

Palabras clave:
Caolín (DD2)
Cuarzo
Residuos de vidrio reciclado

RESUMEN

El presente estudio tiene como objetivo obtener porcelana a partir de materias primas disponibles localmente. Esta porcelana se preparó con la mezcla de caolín, cuarzo, feldespato y residuos de vidrio reciclado. En este trabajo, el costoso feldespato potásico se sustituyó por residuos de vidrio reciclado de vidrio roto de automóviles. Se abordan los efectos de

* *Corresponding author.*
E-mail address: belhouchat_khaled@yahoo.fr (K. Belhouchet).
https://doi.org/10.1016/j.bsecv.2018.05.004

Porcelana
Dureza de Vickers
Propiedades dieléctricas

los residuos de vidrio reciclado que sustituyen parcialmente al feldespato potásico en la elaboración de la porcelana. Los resultados experimentales mostraron efectos importantes de la sustitución de residuos de vidrio reciclado y la temperatura de sinterización sobre las propiedades físicas. Además, la observación de la microestructura mostró que la sustitución del feldespato potásico por los residuos de vidrio reciclado indica que la reducción de la temperatura de cocción de 200 °C se obtuvo con el 30% del peso de adición de vidrio. Aparte de ello, las investigaciones experimentales mostraron excelentes propiedades mecánicas (microdureza) y aislantes (resistencia dieléctrica) de la porcelana preparada en comparación con las de los aislantes de porcelana tradicionales. La microdureza de Vickers encontró un aumento con la adición de vidrio y la temperatura de sinterización. La constante dieléctrica (ε'), la tangente de pérdida dieléctrica (tan δ) y el factor de pérdida (ε") se midieron a diferentes frecuencias. Los resultados revelan que la adición de vidrio mejora las propiedades dieléctricas de las muestras cocidas a 1.100 °C. Finalmente, los mejores resultados del ángulo de fase ∼(-89,2°) se obtuvieron de esta porcelana. Estos resultados demuestran que nuestro aislante preparado es un condensador dieléctrico.

Introduction

In recent years, porcelain is produced in many countries and its technology is well known and described in different textbooks and papers [1]. Although the term porcelain is sometimes applied to a variety of vitreous and near vitreous ware, it is more properly restricted to translucent vitreous ware. A wide range of triaxial ceramic compositions that are used in white ware industries basically contain kaolin, quartz and feldspar [2]. Porcelain insulators and porcelain shells are important equipments in the operation of power plants and transformer substations insulation and supporting wire [3]. Porcelain materials have very interesting properties for many industrial applications. Ceramics possess an extremely low thermal expansion; low thermal conductivity, and high mechanical strength, these properties give an excellent thermal shock resistance [4]. Several reports have been published dealing with crystallization behaviour, microstructure and dielectric properties of many materials prepared by several methods [5,6].

The dielectric properties of porcelain such as dielectric permittivity and the dielectric loss factor depend on the characteristics and relative quantities of different phases [7,8]. Particularly, anorthite and quartz phases tend to reduce the global dielectric loss, whereas mullite increases dielectric loss.

Porcelains also possess low values of dielectric constant ∼(16.4), and dielectric loss factor ∼(0.93), which allow applications in electronic industry such as substrates for instance [9]. Porcelains are generally mixtures of 50 wt% of kaolin, 30 wt% of flux feldspar and 20 wt% of quartz [10–12]. Sintering results in the formation of a composite microstructure with crystals of mullite, relicts of quartz and cristobalite embedded in a glassy matrix [11].

The most established products from waste-derived glasses are feasible by the sintering of pre-stabilized fly ash mixed with clay and recycled soda-lime glass. The sintering treatment does not compromise the chemical stabilization of fly ash, as confirmed by leaching test and by cell culture studies applied on sintered glass-ceramics [12].

Glass-waste interactions were found to provide a homogeneous foaming, without other additives, and partial crystallization. The specific mechanical properties of the resulting cellular glass-ceramics, being comparable to those of conventional porcelain stoneware, sintered above 1100 °C, suggest an extensive use in the building industry [13,14].

Recently, some papers considered the introduction of soda-lime waste glasses as raw materials for both ceramic bodies and glazes [15,16]. In porcelain stoneware bodies, where soda-lime glasses substitute feldspar fluxes, additions of up to 5 wt% do not bring about any significant change in the technological behaviour [17,18]. On this basis, commercial fluxes have been developed as a mixture of feldspar plus different amounts of soda-lime glass and they are currently utilized in porcelain materials. This fact attracts further importance since ceramic industry is classified as heavy industry and consumes huge amounts of diminishing mineral resources [19,20]. In another hand, the use of rock-cutting waste in electrical porcelains manufacture has been investigated [21].

The dielectric properties of the technical porcelain were studied. Consequently, this part is devoted only to the sintering and the dielectric properties of technical porcelains. In the present investigation, preparation of technical porcelains using Algerian raw materials and dielectric properties was carried out. Dielectric constant (ε'), loss factor (ε'') and dielectric loss tangent (tan δ) were studied.

In this work, the improvement of mechanical and dielectric properties of the porcelain insulator sintered at different temperatures has been investigated. To reduce the cost fabrication of these materials, the effects of recycled waste glass in partial replacement of K-feldspar on the crystallization behaviour of porcelain prepared from Algerian kaolin (DD2), quartz and feldspar were also studied.

Materials and methods

White porcelains were prepared from mixtures of four raw materials: kaolin (DD2) [22] from the mine of Djebbel Debbagh in Guelma, Algeria, which is white in colour and enriched in

Table 1 – Chemical compositions of the starting raw materials, mass (%).

Oxides	K (DD2)	Quartz	Feldspar	Recycled waste glass
SiO_2	45.52	99.90	69	70.22
Al_2O_3	38.73	00.03	17.15	01.08
Fe_2O_3	0.04	00.01	00.17	00.08
CaO	00.18	–	02.32	12.01
Na_2O	00.05	–	00.37	13.10
K_2O	00.03	–	10.22	00.03
MgO	–	–	–	01.55
SO_3	–	–	00.16	00.38
L.O.I.	15.44	00.01	00.42	–
Total	99.99	99.95	99.81	98.45

alumina; quartz from Tamanrasset, Algeria, which is white in colour and highly pure; feldspar from Spain (beige in colour and with more than 10% of potassium oxide, its formula is $KAlSi_3O_8$) and waste glass derived from broken car glass. The chemical composition of the starting raw materials as determined by X-ray fluorescence (XRF) is shown in Table 1.

Four compositions were prepared by milling the ready mixed powder according to the batch compositions shown in Table 2. The prepared powder mixtures are named as N00, G10, G20 and G30, where N stands for 0% glass while G stands for glass and 10, 20 and 30 denotes the weight percentage of glass in the composition. Recycled waste glass was added to kaolin and quartz to partially replace potash feldspar. Chemical analysis of feldspar (Table 2) shows that it is a potash feldspar composed mainly of SiO_2. Its K_2O and CaO content is 10.22 wt.% and 2.32 wt.% respectively. The chemical composition of the recycled waste glass reveals that it is composed of high SiO_2 content (70.22%) and similar amounts of CaO (12.01%) and Na_2O (13.10%). Raw materials mixtures were charged into zirconia vials (250 ml in volume) together with zirconia balls (15 units). Milling was performed through a planetary ball mill (Fritsch P6) for 5 hours with a rotation speed of 250 rpm. The slurry was dried at 110 °C, powdered and sieved through a 100 μm mesh and then compacted at a pressure of 100 MPa using a cold uniaxial press. Disc specimens of 13 mm diameter and about 5 mm thickness were shaped. In order to determine an optimum preliminary sintering temperature, the compacts were thermal treated under atmospheric conditions at different temperatures within the range 1000–1300 °C for 2 h of soaking with heating rate of 10 °C/min and cooled down inside the furnace.

XRD analyses were carried out using a Bruker D8 diffractometer. The XRD tests conditions were Ni-filtered Cuk α X radiation (35 kV–30 mA) with a scanning speed of 37° (2θ) per minute and at an increment of 0.05°. Phases identification was achieved by means of the PDF-2 database (ICDD-International Centre for Diffraction Data, New Town Square, PA). The chemical functional groups were investigated by Fourier transform infrared spectroscopy (FT-IR) Perkin Elmer type FT-IR within the wave number range of 4000–400 cm^{-1}. The method described in this study has now been generally adopted with satisfactory results. The substance is finely and smoothly ground under Nujol directly on the KBr pellet and the mull gently pressed between two KBr pellets in order to reduce it to a thin and uniform layer. After recording the spectrum, the pellets are carefully separated, and Nujol is repeatedly washed with very light petroleum ether leaving the fine powder on the surface of the pellets which are then joined again as a sandwich. A second spectrum on the dry powder is then recorded, normally only in the spectral regions masked by the Nujol bands.

All mixtures were subjected to differential thermal analysis (DTA) using Setaram DTA 92 thermal analysis system with 10 °C/min heating rate in air. The bulk density and open porosity of sintered samples sintered at different temperatures were measured using a densimeter model KERN ARS 220-4 and quantified according to Archimedes principle [ISO test method (10545-3)]. Water absorption was estimated by immersion in boiling water, according to recent norms [23].

Linear shrinkage on firing (L.S.%) was evaluated through the equation (ASTM C326):

$$\text{L.S.\%} = \frac{D_1 - D_2}{D_1} \times 100\%, \quad (1)$$

where D_1 and D_2 are the outer diameters of the samples before and after sintering, respectively.

The morphology of fracture surface was observed by scanning electronic microscopy SEM (JEOL JSM-7001F) on samples etched with 10% HF for 30 s.

Vickers micro-hardness (Hv) of sintered samples were determined using a Zwick microhardness tester model 3210 Hv is measured by pressing a rod tip into the material surface and finding the amount of deformation from the dimensions of the formed indenter. A load (P) of 500 g was used; this load was optimized through changing the load from 100 g to 500 g [24]. The time period of the indentation was 12 s immediately after the indentation, the diameters (d) of the formed indents were measured. Hv is quantified using the equation:

$$Hv = 1.8544 \frac{P}{d^2} \quad (2)$$

The dielectric constant (ε'), dielectric loss factor (ε'') and dielectric loss tangent ($\tan\delta$) were measured using a Precision Impedance Analyzer model Wayne Kerr N°6420. In this test, samples of 1.5 mm thickness and 13 mm diameter were used. Samples were inserted between two planar copper electrodes. This capacitor is subjected to an alternating electric field for different frequencies (200 kHz–1 MHz).

Table 2 – Percentage of additive material of samples, mass (%).

Samples	K (DD2)	Quartz	Feldspar	Recycled waste glass
N00	50	20	30	00
G10	50	20	20	10
G20	50	20	10	20
G30	50	20	00	30

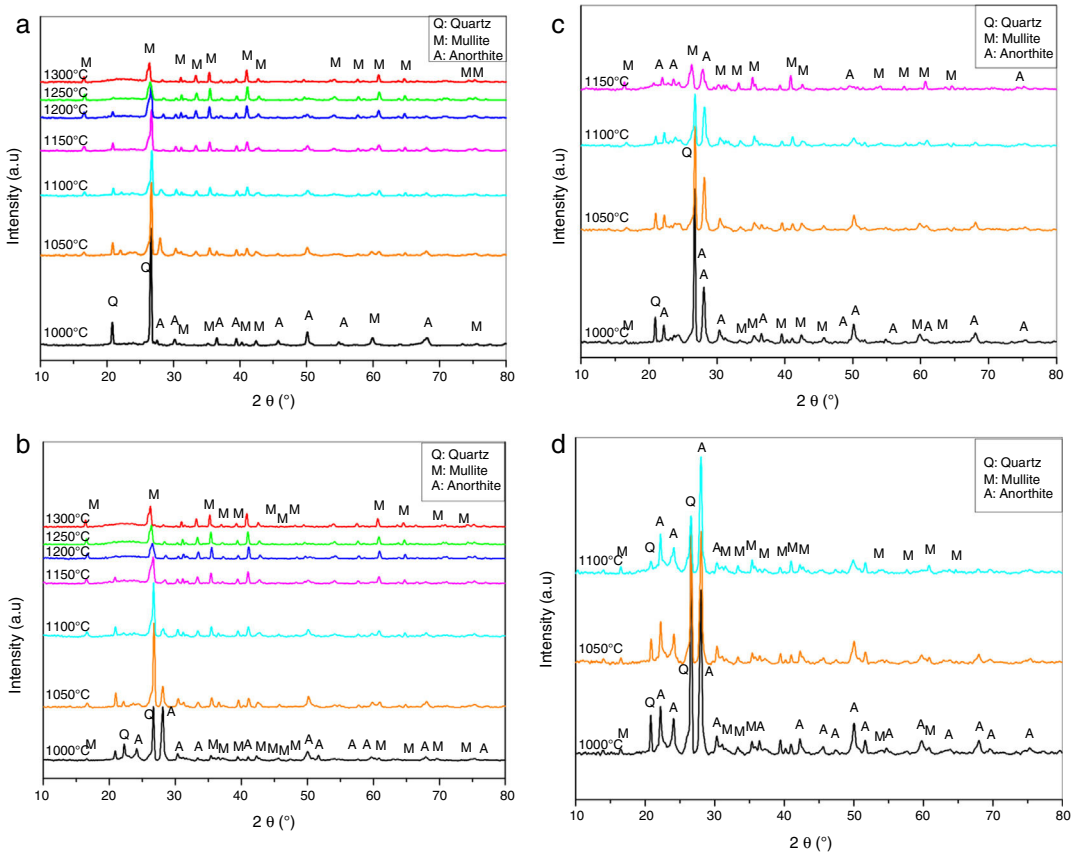

Fig. 1 – XRD patterns of samples sintered at different temperatures for 2 h (a) N00, (b) G10, (c) G20 and (d) G30. Q = quartz, M = mullite, A = anorthite.

Results and discussion

Physical properties

X-rays diffraction patterns obtained from the samples heated at different temperatures are shown in Fig. 1. The XRD diffractogram for N00 sample heat treated at 1000 °C shows the peaks corresponding quartz (PDF#84-0962) and anorthite (PDF#84-0750) (Fig. 1a). At 1050 °C, the dissolution of anorthite and the formation of mullite (PDF#84-0853) as new phase are observed and X-ray patterns of samples fired in the 1150 °C and 1300 °C temperature interval indicates the dissolution of quartz and the development of a glassy phase.

The XRD spectra for the samples G10 (Fig. 1b) shows peaks corresponding to quartz and small peaks corresponding to mullite. From 1050 °C, the presence of a new phase of anorthite is revealed. At 1100 °C the dissolution of anorthite and quartz is observed. A completely dissolution of quartz is noted at 1200 °C. At higher temperature (1250 °C and 1300 °C) the presence of only mullite and glassy phase is observed.

Fig. 1c shows the X-rays diffraction patterns recorded from the samples G20 where a notably decrease in intensity with temperature between 1000 °C and 1300 °C is noticed. At 1000 °C, XRD peaks corresponding to quartz, anorthite and mullite are observed. Anorthite and quartz begins to dissolve from 1100 °C. At 1150 °C, the presence of a glassy phase and mullite were noted.

In the G30 samples (Fig. 1d), three phases of mullite, quartz and anorthite were presented at 1000 °C [21]. The intensity of the peaks corresponding to quartz decreases notably with temperature (1000–1100 °C). At 1100 °C, a glassy phase appears.

The functional groups in porcelain samples synthesized at different temperatures were evaluated by FT-IR as shown in Fig. 2. The spectrum as a whole is divided into two sections;

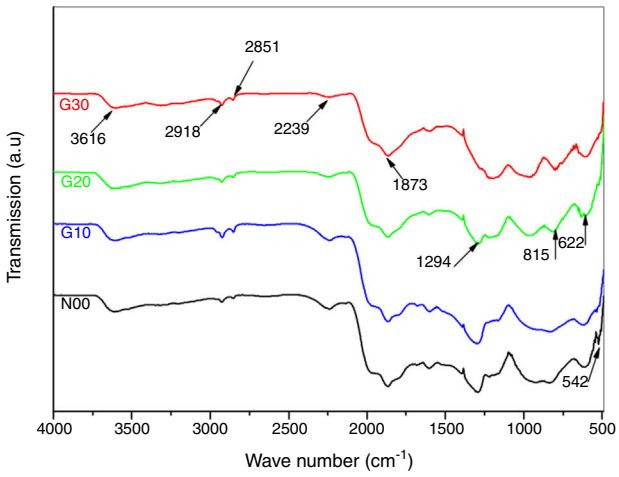

Fig. 2 – FT-IR spectra of the samples sintered at 1100 °C for 2 h.

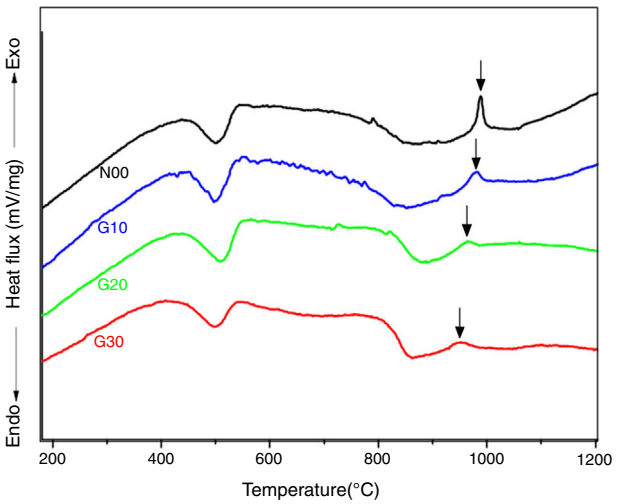

Fig. 3 – DTA curves for samples mixtures during heating.

the first one comprises the main sharp distinctive and characteristic absorption bands extending in the mid IR region. From 500 to about 2000 cm^{-1}, and the second part reveals only two small peaks, at about 2851 and 2918 cm^{-1} followed by a broad band in the far IR region centred at about 3616 cm^{-1}. Moreover, an additional small band around 2239 cm^{-1} is also observed [19,20]. The spectra corresponding to N00 sample heated at 1100 °C reveals the presence of two bands at 515 and 542 cm^{-1} relating to the vibrations of bond Si—O [21,25]. In Fig. 2, the spectra corresponding to N00 and G10 are almost identical. Other bands around 622 and 815 cm^{-1} are attributed to Si—O—Si symmetric stretching of bridging oxygen between tetrahedral. In G20 samples there is a clear modification of the functional groups [26]. A new band at 1294 cm^{-1} corresponding to Si—O in the sample heated at 1100 °C appears [14–21,23–31]. Moreover, the band observed at 1873 cm^{-1} can be related to the asymmetric stretching vibration of CO_3^{2-} anions [23].

The crystallization kinetics of mullite formation in the porcelain may be determined by the DTA technique, which allows to follow the evolution during a continuous heating (isothermal treatment) from ambient temperature to high temperature (1300 °C). DTA curves of studied porcelain samples recorded during heating with a rate of 10 °C/min are shown in Fig. 3. On the curves of all samples, two peaks at about 500 °C and 950 °C are observed. The first one (endothermic) is due to the dehydration of kaolinite, while the second peak (exothermic) is due to spinel formation [30,31]. The first endothermic peak does not experiment any change with addition of feldspar or recycled waste glass, because this peak is related to kaolinite transformation [28]. However both intensity and temperature of the second exothermic peak decrease with recycled waste glass addition from 990 °C to 950 °C for samples N00 and G30, respectively. The proportion of the solvent (CaO, Na_2O (Table 3)) increases with increasing percentage of glass addition, and thus facilitating the formation of spinel phase [24,27].

Fig. 4a represents the bulk density of the pellet disks sintered at various temperatures. It is observed that the bulk density represents a maximum value (2.5 g/cm^3) in all the samples after thermal treatment for 2 h at 1050 °C [32].

Table 3 – Chemical compositions of all samples, mass (%).

Elements	N00	G10	G20	G30
SiO_2	63.44	63.56	63.68	63.81
Al_2O_3	24.49	22.92	21.31	19.70
Fe_2O_3	00.08	00.06	00.05	00.04
CaO	00.79	01.75	02.72	03.69
Na_2O	00.14	01.41	02.68	03.95
K_2O	03.08	02.06	01.04	00.02
MgO	–	00.15	00.31	00.46
SO_3	00.05	00.07	00.16	00.11
L.O.I.	07.85	07.81	07.76	07.72
Total	99.92	99.79	99.71	99.51

For N00 samples, it is seen that the bulk density is practically constant between 1050 °C and 1150 °C. Then, it decreases up to 1200 °C and becomes constant from 1250 °C. This reduction is possibly due to the transformation of residual open porosity into closed porosity and/or the appearance of a new phase (liquid phase) resulting from the presence of K_2O.

In G10 samples, the bulk density is practically constant between 1015 °C and 1150 °C, which is due to the stability of the constituent phases. From 1200 °C, a small decrease in bulk density which is due to the appearance of the liquid phases is observed.

In the case of G20 samples, the bulk density is constant between 1050 °C and 1100 °C and is equal to 2.5 g/cm^3. Then, a linear decrease in the bulk density from 1100 °C to 1250 °C is due to the formation of a liquid phase from the presence of a large amount of different fluxes (K_2O, Na_2O and CaO) (see Table 3). In the case of samples G30, a marked decrease in density can be observed from 1100 °C. This reduction is probably due to the appearance of a large amount of glassy phase. The samples sintered at 1200 °C and 1250 °C show relatively low density values (lower than 1 g/cm^3) due to boiling of the constituent phases [32].

Fig. 4b shows the evolution of the open porosity in porcelain samples according to the sintering temperature. For N00 and

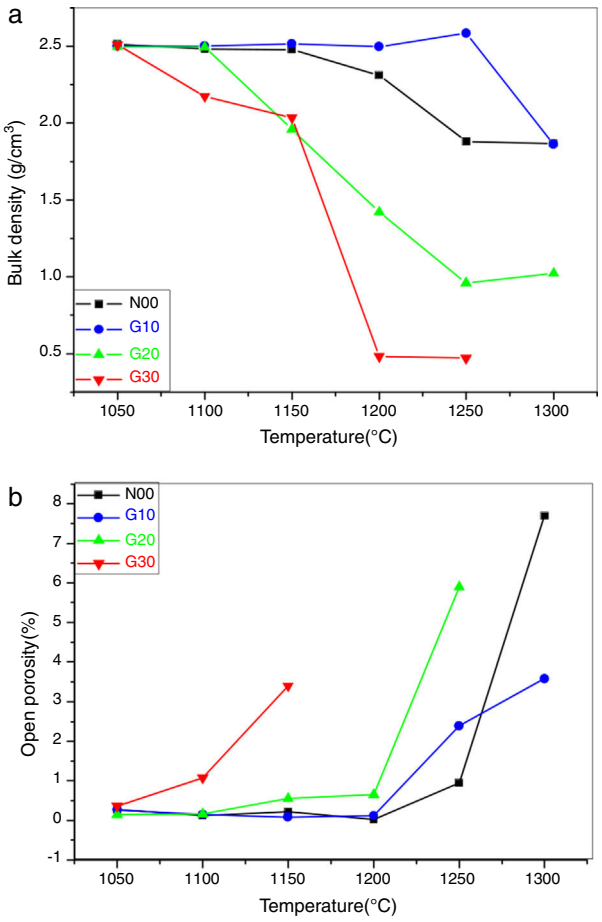

Fig. 4 – (a) Bulk density and (b) open porosity of the samples sintered at different temperatures.

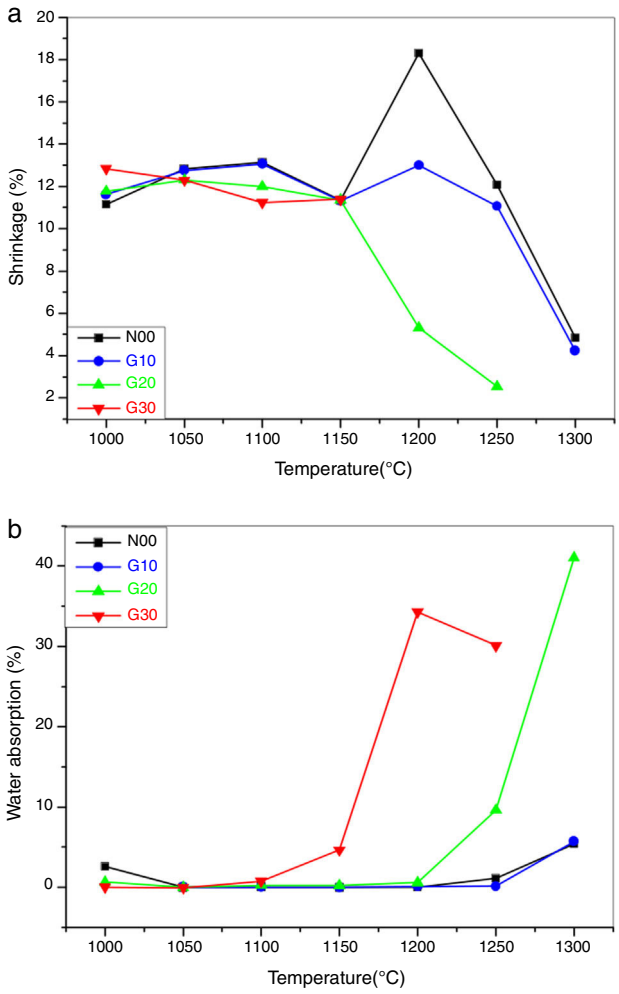

Fig. 5 – (a) Shrinkage and (b) water absorption of the samples sintered at different temperatures.

G10 samples, almost zero values have been detected between 1050 °C and 1200 °C, which indicates the final stage of the sintering process. The appearance of the liquid phase at higher temperature (1250 °C and 1300 °C) permits an easy release of gas trapped in the closed pores, which leads to the formation of new open porosity. The role of the liquid phase in microstructure formation and porosity reduction is not as predominant as in vitrified porcelain [33].

In the case of G20 and G30 samples, an increase of open porosity at 1100 °C and 1150 °C is observed. The decreasing of temperature where open porosity occurs confirms that porosity is due to the presence of liquid phases.

Fig. 5a shows the shrinkage of porcelain samples on firing. All samples show almost constant shrinkage (11–13%) between 1000 °C and 1150 °C. These values are lower than those reported by Kim et al. [34,35]. At 1200 °C, the sample N00 achieves the maximum shrinkage value (18%), which indicates the best sintering temperature. From 1250 °C the decrease in shrinkage is due to the appearance of liquid phases.

Generally, the presence of the liquid phases facilitates the sintering process, but in this case, the existence of a great amount of liquid phase with low density leads to a swelling of the samples. The same remarks were noted for G10 sample.

Regarding G20 samples, a significant reduction in the shrinkage from 1150 °C is due to the presence of the high quantity of the glassy phase. In samples G30, the melting of the materials after 1150 °C (exaggerated swelling) is observed. A high correlation between the shrinkage and bulk density is noted.

Fig. 5b shows the evolution of water absorption of the porcelain samples as a function of temperature. The absorption of water near to zero or very low between 1050 °C and 1250 °C for N00 and G10 samples. This means that the open porosity is completely converted to closed porosity. The appearance of the liquid phase between 1250 °C and 1300 °C causes a swelling of the samples. The release of gases trapped in the closed pores produces a small amount of open porosity. However the absorption of a small amount of water means that the porosity is small.

In the G20 samples, there is a sharp increase in water absorption from 1250 °C. This increase is due to the creation of open porosity. For G30 samples, there is a slight increase in water absorption from 1150 °C. It also means a strong increase at 1200 °C and 1250 °C, which is explained by the creation of a large degree of open porosity. In general, the water absorption is in agreement with the results obtained in open porosity.

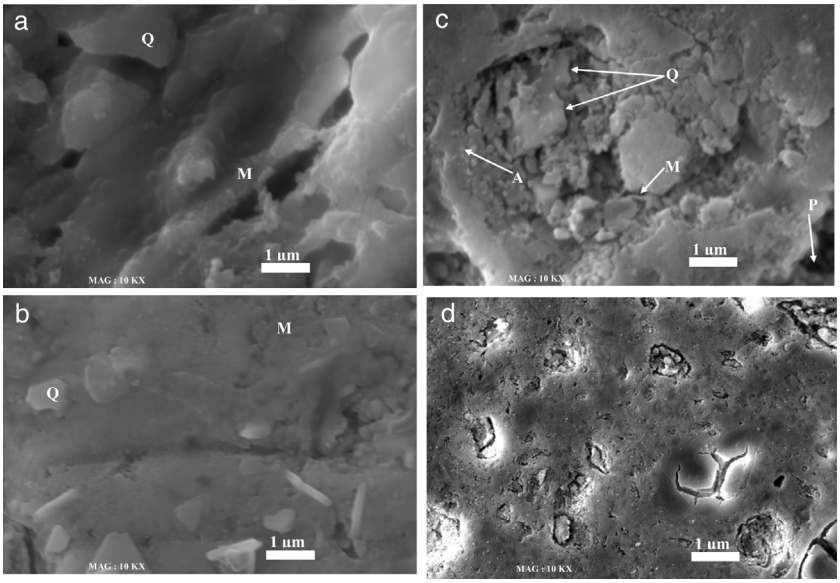

Fig. 6 – SEM micrographs of the samples sintered at 1100 °C for 2 h: (a) N00, (b) G10, (c) G20 and (d) G30. Q = quartz, M = mullite, A = anorthite, P = porosity.

Fig. 6 shows the microstructure of all samples sintered at 1100 °C for 2 h. Based on phase chemical analysis and phase morphology, it was possible to identify the phases named in Fig. 6. All fired samples contain quartz. This residual quartz is retained from the original quartz contained the starting raw materials. In N00 and G10 samples, a well-nigh of quartz grains (randomly form with the vitreous phase) and small grains of mullite are observed as shown in Fig. 6a and b, respectively [36]. In G20 samples, quartz grains are showing different grain sizes, which confirms the relatively good densification of samples sintered at 1100°. In this case multiple phases such as mullite and anorthite were revealed (Fig. 6c). The presence of anorthite was a consequence of the calcium oxide within the waste glass composition. Moreover, the presence of pores is clearly visible in this sample. For the G30 samples (Fig. 6d), a notably change of the microstructure is observed. There are substantial amounts of both crystalline (quartz) and glassy phases. The sample containing glass 20 wt% and sintered at 1100 °C, shows an improvement on the physical behaviour of the insulator.

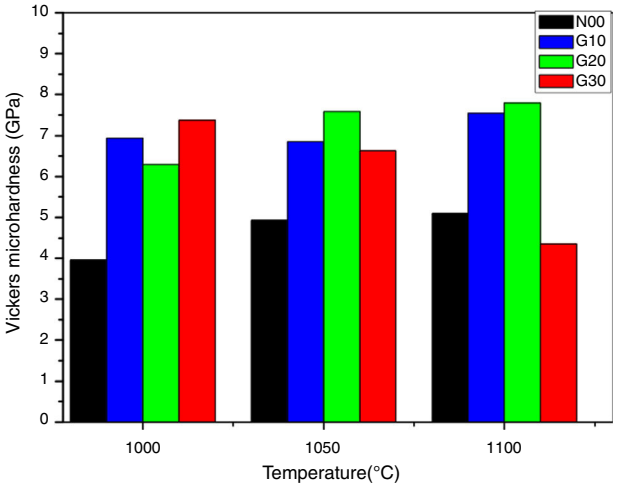

Fig. 7 – Vickers micro-hardness versus the sintering temperatures for samples containing N00, G10, G20 and G30.

Mechanical and dielectric properties

Mechanical properties

The micro-hardness test is an excellent way to evaluate the effect of variables on hardness or resistance to penetration of porcelain samples, mainly after surface etching. This procedure allows the selection of areas free of porosities and allows indentations on heterogeneous areas.

The procedure allows determining the Vickers hardness (*Hv*). It is known from the literature [37] that the produced impression dimension is related to the applied load according to the hardness of the material.

Fig. 7 shows the Vickers micro-hardness (*Hv*) as function of sintering temperatures. The Vickers hardness values increased from 4 to 8 GPa as the sintering temperatures between (1000 °C and 1100 °C) and it is influenced by glass additions. The existence of mullite increases the micro hardness of porcelain (mullite hardness ≈ 15 GPa) [38,39].

It is observed that the addition of glass in porcelain composition leads to an increase in micro hardness values. For G10 and G20 samples, the micro-hardness increase by 33% and 38% respectively, in relation to the reference porcelain sample N00 sintered at 1100 °C. The increase in both mullite content and bulk density resulting from glass addition porcelain contribute to this improvement. Mullite is considered a key phase during the formation of the porcelain [40]. According to XRD patterns, the concentration of mullite increases by adding glass. The concentration of any phase is related to the intensity of their peaks [41]. It can be observed also that G30 sample

(containing glass instead of Feldspar) sintered at 1000 °C shows a high micro-hardness value, which decreases in sample prepared at 1100 °C. This is due to a higher densification at 1000 °C, which is followed of an increase in residual porosity as temperature increases. However, the micro-hardness values of G10 and G20 samples are approximately constant at the limit of 8 GPa. This is due to presence of feldspar and glass (K_2O, Na_2O) in the original raw material mixture since these fluxing elements facilitate the sintering process and eliminate the residual porosity.

The addition of glass has a positive effect on mechanical properties. The optimal Vickers micro-hardness (8 GPa) is observed in G20 sample thermal treated at 1100 °C. This value is relatively raised when compared to that (6.5 GPa) obtained by [41,42] but near to that (8.5 GPa) reported by [43]. The variation of mechanical properties is mainly related to the vitrification degree and residual porosity [44]. The number of topological constraints between atoms or crystalline phases in the porcelain has an impact on hardness of a material containing a glassy or liquid phase.

Porcelain is characterized by its high ability to dielectric isolation due to the strong bonding between its atoms. The bonds between porcelain atoms are ionic bonds of high durability. This is because the ionic bond possesses electrostatic energy as well as the valence electrons that are strongly interconnected in covalent bonds.

Feldspar is one of the most important materials that improve the properties of the mechanical porcelain product, but its increase negatively affects the insulation and the properties of porcelain are affected by the concentration and quality of oxides (Na^+, K^+) for containing alkali metal ions [45]. Developing an insulator having excellent mechanical strength was realized. The composition has 20 wt% sintered at 1100 °C found to be most suitable for mechanical applications.

Dielectric properties

In this study, the dielectric values were improved by adding a glass content of 20 wt% in the base composition. A change of dielectric properties as function of both; conditions of the manufacture of the porcelain body and conditions of measuring was observed, the dependence of dielectric constant (ε'), dielectric loss factor (ε'') and dielectric loss tangent (tan δ) on the frequency (f) is shown in Fig. 8a,b and Fig. 9, respectively. It is noted that N00 and G20 samples sintered at 1100 °C show a slight decrease and relative stability of the dielectric constant (ε') with the increase in the frequencies as shown in Fig. 8a. This is due to the decrease in the polarization of the space charges. The stability of the dielectric constant (ε') at high frequencies means that the effect of space charge was suppressed [29]. On further addition of glass, the dielectric constant value decreases for G20 sample compared with N00 values when measured within the frequency range of 200 kHz–1 MHz (Fig. 8a).

Fig. 8b shows the dielectric loss factor (ε'') as function of frequency (Hz). It is clearly shown that N00 and G20 samples sintered at 1100 °C show a reduction of dielectric loss factor (ε'') values when measured within the frequency range of 200 kHz–1 MHz. After that a stability of loss factor values is noted. The results concerning the loss factor values are approximately similar to those reported by several authors [36,46].

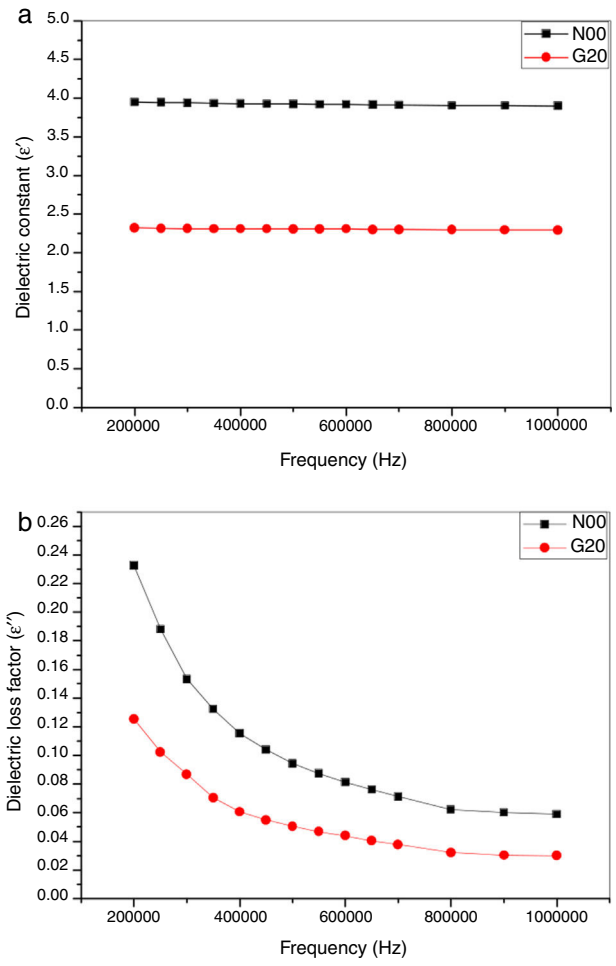

Fig. 8 – (a) Dielectric constant (ε'), and (b) dielectric loss factor (ε'') versus frequency (Hz).

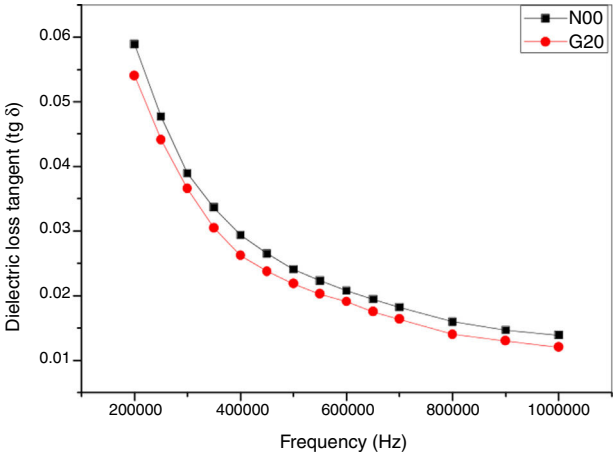

Fig. 9 – Dielectric loss tangent (tan δ) versus frequency (Hz).

Fig. 9 shows the dielectric loss tangent (tan δ) as function of frequency (Hz). A decrease of (tan δ) is found within the range of 200 kHz–1 MHz. These values are also approximately similar

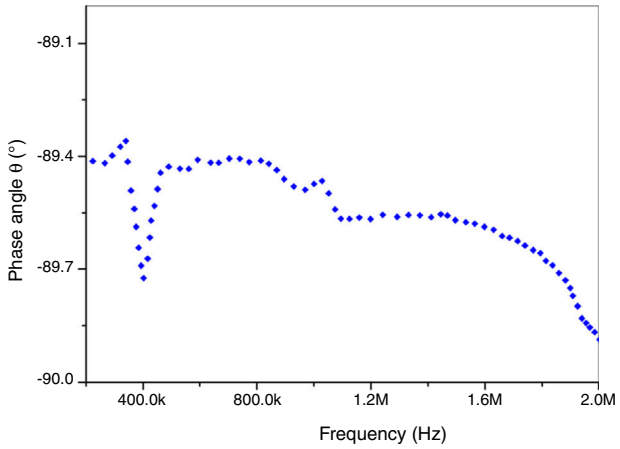

Fig. 10 – Phase angle θ (°) versus frequency (Hz).

to values archived by [40,47]. A minor improvement of (tan δ) by adding glass (G20) is reported.

It is known that the dielectric constant of porcelain increases in presence K^+ and Na^+ cations [46] and decreases when they are replaced by Ca^{2+}, Mg^{2+}, and Ba^{2+} cations [45]. These dielectric properties decrease with the glass addition. Thus, G20 sample showed a 31.02% of improvement in relation of the reference porcelain sample (N00) at high frequency. Glass phase has a dominant influence on electrical and dielectric properties of fired ceramics. These properties are determined by the concentration and mobility of K^+ and or Na^+ ions in this phase [48]. On the other hand, mullite has a vital role on dielectric properties. XRD analyses indicated that samples with added glass showed higher percentage of crystalline phases than classic porcelain without glass addition, which can explains the improvement of dielectric strength.

Fig. 10 shows phase angle (θ) as function of frequency (Hz). A significant decrease of phase angle values was observed with increasing frequencies. It brings near to (−89.2°). It is important to notify that this result proves that our prepared insulator is a capacitor circuit. This porcelain sample is suitable for application as electrical insulators in the present form because of its higher dielectric.

Conclusions

The use of recycled waste glass powder as a fluxing agent replacing feldspar in this work led to a lower sintering temperature of porcelain samples, which was explained by a higher amount of fluxing elements compared to feldspar. XRD analyses show the formation of porcelain bodies with mullite and quartz phases in N00 sample, and anorthite is also found in G10, G20 and G30 samples. From this investigation, the possibility of preparing white porcelain from kaolin, quartz and recycled waste glass (for feldspar replacement) was lighted. This work demonstrated that mechanical and dielectric properties of porcelain prepared at low temperature are improved by glass addition.

The added glass, which is responsible for the improvement in the Vickers micro-hardness as well as the dielectric constant value, was selected in G20 sample sintered at 1100 °C. The low dielectric constant provides the advantage of using the insulator in high voltage (capacitor dielectrics). Finally, the obtained results propose extremely interesting properties for high voltage insulation domain.

REFERENCES

[1] A. Karamanov, E. Karamanova, A. Ferrari, F. Ferrante, M. Pelino, The effect of fired scrap addition on the sintering behavior of hard porcelain, J. Ceram. Int. 32 (2006) 727–732.
[2] S. Bhattacharyya, K.S. Das, N.K. Mitra, Effect of titania on fired characteristics of triaxial porcelain, J. Bull. Mater. Sci. 28 (2005) 445–452.
[3] L. Chen, J.Q. Wang, Related problems in ultrasonic detection of porcelain insulator, in: The 17th world conference on non conductive testing, Shanghai, China, J. Int. Proc. (2008).
[4] F. Matteucci, M. Dondi, G. Guarini, Effect of soda-lime glass on sintering and technological properties of porcelain stoneware tiles, J. Ceram. Int. 28 (2002) 873–880.
[5] M. Mumtaz, A. Liaqat, S. Azeem, S. Ullah, G. Hussain, M.W. Rabbani, K. Abdul Jabbar Nadeem, Dielectric properties of (Zn)x/CuTl-1223 nanoparticle–superconductor composites, J. Adv. Ceram. 5 (2) (2016) 159–166.
[6] C. Rafael Cena, A. Kumar Behera, B. Behera, Structural, dielectric and electrical properties of lithium niobate microfibers, J. Adv. Ceram. 5 (1) (2016) 84–92.
[7] B. Kumar Paul, K. Haldar, D. Roy, B. Bagchi, A. Bhattacharya, S. Das, Abrupt change of dielectric properties in mullite due to titanium and strontium incorporation by sol–gel method, J. Adv. Ceram. 3 (4) (2014) 278–286.
[8] C.R. Gautam, A. Madheshiya, R. Mazumder, Preparation, Crystallization, microstructure and dielectric properties of lead bismuth titanate borosilicate glass ceramics, J. Adv. Ceram. 3 (2014) 194–206.
[9] J.J. Liang, Q.H. Lin, X. Zhang, T. Jin, Y.Z. Zhou, X.F. Sun, B.G. Choi, I.S. Kim, J.H. Do, C.Y. Jo, Effects of alumina on cristobalite crystallization and properties of silica-based ceramic cores, J. Mater. Sci. Technol. 33 (2016) 204–209.
[10] S. Yuruyen, H.O. Toplan, The sintering kinetics of porcelain bodies made from waste glass and fly ash, J. Ceram. Int. (35) (2009) 2427–2433.
[11] W.M. Carty, U. Senapati, Porcelain-raw materials, processing, phase evolution and mechanical behavior, J. Am. Ceram. Soc. 81 (1998) 3–20.
[12] I. Ponsot, E. Bernardo, E. Bontempi, L. Depero, R. Detsch, R.K. Chinnam, A.R. Boccaccini, Recycling of pre-stabilized municipal waste incinerator fly ash and soda-lime glass into sintered glass-ceramics, J. Clean. Prod. 89 (2015) 224–230.
[13] I. Ponsot, E. Bernard, Self glazed glass ceramic foams from metallurgical slag and recycled glass, J. Clean. Prod. 59 (2013) 245–250.
[14] A. Tucci, L. Esposito, E. Rastelli, C. Palmonari, E. Rambaldi, Use of soda-lime scrap-glass as a fluxing agent in a porcelain stoneware mix, J. Eur. Ceram. Soc. 24 (2004) 83–92.
[15] N. Marinoni, D. D'alessio, V. Diella, A. Pavese, F. Francescon, Effects of soda-lime-silica waste glass on mullite formation kinetics and micro-structures development in vitreous ceramics, J. Environ. Sci. Manage. 124 (2013) 100–107.
[16] J. Qin, C. Cuin, X. Hussain Cui, A. Yang, C.S. Yang, Recycling of limemud and fly ash for fabrication of anorthite ceramic at low sintering temperature, J. Ceram. Int. 41 (2015) 5648–5655.
[17] A. Tucci, E. Rambaldi, L. Esposito, Use of scrap glass as raw material for Porcelain stoneware tiles, J. Adv. Appl. Ceram. 105 (2006) 40–45.
[18] A. Karamanov, M. Pelino, M. Slavo, I. Metekovits, Sintered glass ceramics from incinerator fly ashes. Part II. The

influence of particle size and heat-treatment on the properties, J. Eur. Ceram. Soc. 23 (2003) 1609–1615.
[19] H.A. Seung-Ryong, K. Sung-Hun, L. Jai-Bong, H. Jung-Suk, Y. In-Sung, Improving shear bond strength of temporary crown and fixed dental prosthesis resins by surface treatments, J. Mater. Sci. 51 (2016) 1463–1475.
[20] E. Bernardo, Y. Pontikes, G.N. Angelopoulos, Optimization of low temperature sinter crystallization of waste derived glass, J. Adv. Appl. Ceram. 111 (2012) 472–479.
[21] H.R. Fernandes, J.M.F. Ferreira, Recycling of chromium-rich leather ashes in porcelain tiles production, J. Eur. Ceram. Soc. 27 (2007) 657–4663.
[22] F. Chouia, H. Belhouchet, F. Sahnoune, F. Bouzrara, Reaction sintering of kaolin-natural phosphate mixtures, J. Ceram. Int. 41 (2015) 8064–8069.
[23] ISO 10545-3, Ceramic Tiles—Part 3: Determination of Water Absorption, Apparent Porosity, Apparent and Relative Density and Bulk Density, 1997.
[24] M. Heraiz, F. Sahnoune, H. Belhouchet, N. Saheb, Synthesis of Al_2O_3 containing mullite from Algerian kaolin and boehmite, J. Optoelectron. Adv. Mater. 15 (2013) 1263–1267.
[25] V.S. Nandi, F. Raupp-Pereira, O.R.K. Montedo, A.P.N. Oliveira, The use of ceramic sludge and recycled glass to obtain engobes for manufacturing ceramic tiles, J. Clean. Prod. 86 (2015) 461–470.
[26] E. Khalil, F.H. El Batal, Y. Hamdy, H. Zidan, M. Aziz, A. Abdelghany, Infrared absorption spectra of transition metals-doped soda lime silica glasses,.J Phys. B 405 (2010) 1294–1300.
[27] A.J. Souza, B.C.A. Pinheiro, J.N.F. Holanda, Recycling of gneiss rock waste in the manufacture of vitrified floor tiles, J. Environ. Manage. 91 (2010) 685–689.
[28] S.R. Braganca, C.P. Bergmann, Waste glass in porcelain, J. Mater. Res. 8 (2005) 39–44.
[29] W. Shunhua, W. Xuesong, W. Xiaoyong, Y. Hongxing, G. Shunqi, Effect of Bi_2O_3 additive on the microstructure and dielectric properties of $BaTiO_3$-based ceramics sintered at lower temperature, J. Mater. Sci. Technol. 26 (2010) 472–476.
[30] S.Q. Yang, P. Yuan, H.P. He, Z.H. Qin, Q. Zhou, J.X. Zhu, D. Liu, Effect of reaction temperature on grafting of γ-aminopropyl triethoxysilane (APTES) onto kaolinite, J. Appl. Clay Sci. 62 (2012) 8–14.
[31] A.A. Wereszczak, K. Breder, M.K. Ferber, T.P. Kirkland, E.A. Payzant, C.J. Rawn, E. Krug, C.L. Larocco, R.A. Pietras, M. Karakus, Dimensional changes and creep of silica core ceramics used in investment casting of superalloys, J. Mater. Sci. 37 (2002) 4235–4245.
[32] I.M. Bakr, Effect of waste glass and zircon on ceramic properties and microstructure of porcelain tiles, J. Adv. Appl. Ceram. 104 (2005) 243–248.
[33] S. Maity, B.K. Sarkar, Development of high-strength whiteware bodies, J. Eur. Ceram. Soc. 16 (1996) 1083–1088.
[34] K. Kim, J. Hwang, LCD waste glass as a substitute for feldspar in the porcelain sanitary ware production, J. Ceram. Int. 41 (2015) 7097–7102.
[35] E. Bernardo, P.A. Bingham, Sintered silica phosphate glass ceramics from MBM ash and recycled soda-lime-silica glass, J Adv Appl Ceram. 110 (2011) 41–48.
[36] M. Awaad, S. Naga, M.N. EL-Mehalawy, Effect of replacing weathered feldspar for potash feldspar in the production of stoneware tiles containing fish bone ash, J. Ceram. Int. 41 (2015) 7816–7822.
[37] N. Montoya, F. Serrano, M. Reventós, J.M. Amigo, J. Alarcón, Effect of TiO_2 on the mullite formation and mechanical properties of alumina porcelain, J. Eur. Ceram. Soc. 30 (2010) 839–846.
[38] P. Ramaswamy, S. Vynatheya, S. Seetharamu, Significance of structure–property relationship in alumina based porcelain insulators to achieve quality, Bull. J. Mater. Sci. 28 (2005) 681–688.
[39] L. Sidjanin, D. Rajnovica, J. Ranogajec, E. Molnar, Measurement of Vickers hardness on ceramic floor tiles, J. Eur. Ceram. Soc. 27 (2007) 1767–17773.
[40] F. Muthafar, B. Al-Hillin, T. Kalid, C. Al-Rasoul, Characterization of alumino-silicate glass/kaolinite composite, J. Ceram. Int. 39 (2013) 5855–5862.
[41] F. Muthafar, B. Al-Hilli, T. Kalid, C. Al-Rasoul, Influence of glass addition and sintering temperature on the structure, mechanical properties and dielectric strength of high-voltage insulators, J. Mater. Des. 31 (2010) 3885–3890.
[42] R. Santos, F.S. Silva, R.M. Nascimento, F.V. Motta, J.C. Souza, B. Henriques, The mechanical properties and microstructure of zirconia-reinforced feldspar-based porcelain, J. Ceram. Int. 42 (2016) 14214–14221.
[43] A. Yunlong, X. Xianghua, H. Wen, L. Bingliang, F. Yaqi, Microstructure and properties of $Al_2O_3(n)/ZrO_2$ dental ceramics prepared by two-step microwave sintering, J. Mater. Des. 65 (2015) 1021–1027.
[44] K. Alexander, K. Emilia, M.F. Anna, F. Fabiola, P. Mario, The effect of fired scrap addition on the sintering behavior of hard porcelain, J. Ceram. Int. 32 (2006) 727–732.
[45] V.P. Ll'ina, Feldspar material from Karelia for electrical engineering, J. Glass Ceram. 61 (2004) 195–197.
[46] Y. Ling, L. Richard, B. Nicholas, P. Zhongxiao, S. Richard, Damage morphology produced in low-cycle high-load indentations of feldspar porcelain and leucite glass ceramic, J. Mater. Sci. 4 (2013) 101–107.
[47] S.P. Chaudhuri, P. Sarkar, Dielectric behaviour of porcelain in relation to constitution, J. Ceram. Int. 26 (2000) 865–875.
[48] V. Tmovcova, I. Fura, F. Hanic, Influence of technological texture on electrical properties of industrial ceramics, J. Phys. Chem. Sol. 68 (2007) 1135–1139.